Reaction Pathway for Inhibition of Blood Coagulation Factor Xa by Tick Anticoagulant Peptide

Susan P. Jordan, Shi-Shan Mao, Sidney D. Lewis, and Jules A. Shafer*
Biological Chemistry Department, Merck Sharp & Dohme Research Laboratories, West Point, Pennsylvania 19486
Received November 25, 1991; Revised Manuscript Received March 30, 1992

ABSTRACT: The reaction pathway for inhibition of human factor Xa (fXa) by recombinant tick anticoagulant peptide (rTAP) was studied by stopped-flow fluorometry. In the presence of the fluorogenic substrate *N-tert*-butyloxycarbonyl-L-isoleucyl-L-glutamylglycyl-L-arginyl-7-amido-4-methylcoumarin (B-IEGR-AMC) and under pseudo-first-order conditions, inhibition appears to occur via a two-step process. Initially, a weak enzyme–inhibitor complex forms with a dissociation constant (K_i) of 68 ± 6 μM. The initial complex then rearranges to a more stable fXa–rTAP complex with a rate constant (k_2) of 123 ± 5 s^{-1}. The apparent second-order rate constant (k_2/K_i) describing formation of the stable complex is (1.8 ± 0.2) × 10^6 M^{-1} s^{-1}. Studies of the reaction of rTAP with fXa in the presence of the fluorescent active-site probe *p*-aminobenzamidine (P) revealed a reaction pathway wherein rTAP initially binds to the fXa–P complex in a two-step process prior to displacing P from the active site. These results indicate that rTAP can bind fXa via a site distinct from the active site (an exosite). The subsequent displacement of P from the active site of fXa by rTAP exhibits a dependence on the concentration of P, indicating that rTAP is locked into the active site in a third step. Consistent with the existence of a fXa exosite, an active-site-blocked derivative of fXa (DEGR-fXa) was shown to form a complex with rTAP with a dissociation constant of 5.9 ± 0.7 μM. Since the action of rTAP on fXa appeared to be similar to that of r-hirudin on thrombin, the ability of rTAP and r-hirudin to inhibit α-thrombin and fXa, respectively, was assessed. K_i's of 26 μM and ~3 mM were measured for the inhibition of α-thrombin and fXa by rTAP and r-hirudin, respectively.

The serine protease factor Xa (fXa)[1] is a pivotal protein in blood coagulation that functions at the intersection of the intrinsic and extrinsic coagulation pathways. Together with Ca^{2+}, phospholipid, and its protein cofactor factor Va, fXa cleaves prothrombin to thrombin which in turn converts fibrinogen to fibrin, the insoluble matrix of blood clots. The pivotal position for fXa in blood coagulation suggests that inhibitors of fXa may have therapeutic potential as antithrombotic agents. One such inhibitor of fXa, tick anticoagulant peptide (TAP), recently isolated from the tick *Ornithodoros moubata* (Waxman et al., 1990), is a 60 amino acid protein with 3 cystinyl disulfide bonds (Sardana et al., 1991). Expression of TAP (rTAP) in yeast (*Saccharomyces cerevisiae*) has yielded sufficient quantities of rTAP for characterization of its pharmacological properties and its interactions with fXa (Neeper et al., 1990).

Previous studies with rTAP have shown that it is a tight-binding, competitive inhibitor of fXa (Jordan et al., 1990). Although it has limited structural homology with the Kunitz class of serine protease inhibitors, its mode of action more closely resembles that of the thrombin inhibitor hirudin, which has been isolated from the leech *Hirudo medicinalis* (Markwardt, 1970). This 65 amino acid protein also contains 3 disulfide bonds. Whereas hirudin is specific for α-thrombin and rTAP is specific for fXa, both inhibitors bind very tightly to their respective target enzymes, and, in contrast to the Kunitz inhibitors, neither inhibitor appears to be cleaved during the inhibition process (Stone & Hofsteenge, 1986; Jordan et al., 1990). Hirudin has been found to interact with α-thrombin at both the active site and a fibrinogen-binding site of α-thrombin (an exosite) that is distinct from the active site (Stone & Hofsteenge, 1986; Stone et al., 1987; Naski et al., 1990). Prior to the present study, however, there has been no evidence for the involvement of an exosite in the interactions of fXa. The previously published information concerning the reaction of rTAP and fXa, although consistent with a simple one-step reaction (Scheme I), does not exclude a more complex reaction pathway.

Scheme I

$$E + I \underset{k_{-1}}{\overset{k_1}{\rightleftharpoons}} EI$$

In the present study, we employed stopped-flow spectrometry to characterize the inhibition of fXa by rTAP in greater detail, and demonstrated the existence of a multistep pathway for the inhibition of fXa by rTAP, wherein rTAP interacts with fXa at both the active site of fXa and a site distinct from the active site (an exosite).

Experimental Procedures

Materials. The fluorogenic substrate *N-t*-Boc-Ile-Glu-Gly-Arg-7-amido-4-methylcoumarin (B-IEGR-AMC) was purchased from Sigma, dissolved in double-distilled water, and filtered (0.2 μm). Its concentration was determined in water using an ϵ_{325} = 1.72 × 10^4 M^{-1} cm^{-1}. The fluorescent probe *p*-aminobenzamidine (P) was purchased from Aldrich, and its concentration was determined in water using an ϵ_{293} = 15000 M^{-1} cm^{-1} (Olson & Shore, 1982). Dansyl-L-glutamylglycyl-L-arginine chloromethyl ketone (DEGR-CK) was

* To whom correspondence should be addressed.

[1] Abbreviations: B-IEGR-AMC, *N-tert*-butyloxycarbonyl-L-isoleucyl-L-glutamylglycyl-L-arginyl-7-amido-4-methylcoumarin; DEGR-CK, dansyl-L-glutamylglycyl-L-arginine chloromethyl ketone; DEGR-fXa, active-site histidine derivative of human factor Xa obtained by reaction of human fXa with DEGR-CK; DMSO, dimethyl sulfoxide; FMGB, fluorescein mono-*p*-guanidinobenzoate; Chromozym TH, tosyl-Gly-Pro-Arg-*p*-nitroanilide; fXa, human factor Xa; P, *p*-aminobenzamidine; PEG 8000, poly(ethylene glycol) 8000; TAP, tick anticoagulant peptide; rTAP, recombinant tick anticoagulant peptide; r-hirudin, recombinant hirudin; TBS, Tris-buffered saline.

0006-2960/92/0431-5374$03.00/0

purchased from Calbiochem. The chromogenic substrate of fXa, Tosyl-Gly-Pro-Arg-*p*-nitroanilide (Chromozym TH), was purchased from Boehringer Mannheim. The chromogenic substrate of α-thrombin, Sar-Pro-Arg-*p*-nitroanilide, was purchased from Sigma. All other reagents were of analytical grade.

Human fXa (fXa) was prepared from human factor X (Haematologic Technologies) by the method of Bock et al. (1989) or was purchased directly from Enzyme Research Laboratories, Inc., or Haematologic Technologies, Inc. FXa concentrations were determined using an $\epsilon_{280}^{1\%} = 11.6$ and a molecular weight of 46 000 (Di Scipio et al., 1977a,b). The protein was homogeneous as judged by sodium dodecyl sulfate gel electrophoresis under reducing conditions in the Laemmli buffer system (Laemmli, 1970), and active-site concentrations were determined by titration with fluorescein mono-*p*-guanidinobenzoate (FMGB) (Bock et al., 1989). DEGR-fXa either was purchased from Haematologic Technologies, Inc., or was prepared by incubating DEGR-CK with fXa (2.5:1 molar ratio) for 90 min at room temperature followed by overnight dialysis versus 20 mM Tris-HCl, pH 7.4, containing 150 mM NaCl (TBS) at 4 °C. The resulting DEGR-fXa was determined to have an enzymatic activity less than 0.01% of that of fXa. The concentration of DEGR-fXa was determined using an $\epsilon_{335} = 6.3 \times 10^3$ M^{-1} cm^{-1} (Husten et al., 1987). Recombinant tick anticoagulant peptide (rTAP) was prepared as previously described (Neeper et al., 1990). rTAP protein concentrations were determined either by quantitative amino acid analysis or by using an $\epsilon_{280} = 1.78 \times 10^4$ M^{-1} cm^{-1} obtained by the method of Gill and von Hippel (1989). r-Hirudin concentration was determined by quantitative amino acid analysis. α-Thrombin was the generous gift of Dr. John W. Fenton, II. The concentration of α-thrombin was determined using $\epsilon_{280}^{1\%} = 18.3$ in 0.1N NaOH and a molecular weight of 36 500 (Fenton et al., 1977).

Studies of Rapid Reactions. These were performed using a Kinetics Instruments stopped-flow spectrofluorometer (dead time = 1.2 ms) interfaced with an OLIS 4300S data system (On-Line-Instrument-Systems, Jefferson, GA) and an Applied Photophysics sequential stopped-flow spectrometer DX.17MW interfaced with an Archimedes 420/I computer. The values of rate constants reported represent averages of 4–8 runs. Unless otherwise stated in the text, all reactions were performed at 25 °C in TBS containing 0.1% PEG-8000 (reaction buffer). In studies which utilized *p*-aminobenzamidine (P) as a probe, P was excited at 330 nm using a 345-nm cutoff fluorescence emission block (Oriel Corp.). Samples in which the hydrolysis of B-IEGR-AMC substrate was monitored were excited at 380 nm using a 400-nm cutoff fluorescence emission block.

Unless otherwise indicated, substrate hydrolysis experiments were performed under pseudo-first-order conditions (i.e., [rTAP] $\gg$ [fXa], [B-IEGR-AMC] $\gg$ [fXa], and [B-IEGR-AMC] $\ll K_m$). rTAP (0.1–300 μM initial concentration) was premixed with B-IEGR-AMC (60 μM initial concentration) prior to being reacted with an equal volume of fXa (0.01–4 μM initial concentration, and [fXa] $\leq$ 0.1 [rTAP]) in the stopped-flow spectrofluorometer. The reactions were monitored for at least 8–10 half-lives of k'_{obs} at each concentration of inhibitor. This method for evaluating rate constants for inactivation of an enzyme by continuously monitoring substrate turnover has been described by Zhou et al. (1989) and Tian and Tsou (1982) in which the data were analyzed by fitting the data to an integrated first-order rate equation:

$$F = V_s t + [(V_0 - V_s)/k'_{obs}][1 - \exp(-k'_{obs} t)] + F_0 \quad (1)$$

F_0, F, V_0, and V_s represent the initial fluorescence, the fluorescence at time t, and the initial and final rates of change of fluorescence, respectively. The value of k'_{obs} in eq 1 is related to the pseudo-first-order rate constant for inhibition, k_{obs}, by

$$k_{obs} = k'_{obs}(K_m + [S])/K_m \quad (2)$$

Pseudo-first-order conditions were also maintained for studies in which *p*-aminobenzamidine was used as an active-site probe. These data were analyzed using the software packages which included exponential curve-fitting equations. In this case, the probe (200 μM) was premixed with an equal volume of fXa (0.1–1 μM, with [fXa] $\leq$ 0.1[rTAP]) followed by equilibration at 25 °C for 5–20 min, prior to reaction with an equal volume of a solution of rTAP (1–200 μM) in the stopped-flow spectrofluorometer. Studies in which the concentration of P was varied while those of rTAP and fXa remained constant were performed in a similar manner with fXa (1 μM) and P (20–800 μM) being preincubated in reaction buffer prior to the addition of an equal volume of rTAP (10 μM) in the Kinetics Instruments stopped-flow spectrometer.

Interaction of DEGR-fXa with rTAP. The effect of preincubation of excess DEGR-fXa with rTAP on the rate constant for subsequent reaction of the rTAP with fXa was analyzed to characterize the binding of rTAP to DEGR-fXa. Solutions containing 100 nM rTAP were preincubated at 25 °C (1–4 h) with increasing concentrations of DEGR-fXa (5–100 μM) and B-IEGR-AMC substrate (60 μM) prior to being mixed with an equal volume of 10 nM fXa in the stopped-flow spectrofluorometer. The fluorescence (excitation at 380 nm) was monitored using a 400-nm cutoff filter, and the rate constant (k_{obs}) for inhibition of fXa by rTAP was determined by fitting the curves by nonlinear regression to eq 8 in the text. Control reactions were performed in the absence of DEGR-fXa to determine the intrinsic rate constant for reaction of rTAP with fXa.

Specificity of rTAP and r-Hirudin. The inhibition of α-thrombin-catalyzed hydrolysis of 16 μM Sar-Pro-Arg-*p*-nitroanilide (K_m = 175 μM) at 37 °C by rTAP was measured in solutions containing 50 mM Tris, pH 7.4 (37 °C), 150 mM NaCl, and 0.1% PEG 8000 at the indicated concentrations of rTAP. Initial rates were determined from the time-dependent increases in absorbance at 405 nm. Control experiments showed that the initial rates were independent of the time of preincubation of rTAP with α-thrombin under the experimental conditions. The inhibition of fXa-catalyzed hydrolysis of 16 μM Chromozym TH (K_m = 158 μM) at 37 °C by r-hirudin was measured in solutions containing 50 mM Tris, pH 7.4 (37 °C), 150 mM NaCl, and 0.1% PEG 8000 at the indicated concentrations of r-hirudin.

Results

Kinetics Parameters for the Interaction of fXa with rTAP. The inhibition of serine proteinases by protein inhibitors is often described by either Scheme I or Scheme II (Leytus et al., 1984).

Scheme II

$$E + I \underset{k_{-1}}{\overset{k_1}{\rightleftharpoons}} EI \underset{k_{-2}}{\overset{k_2}{\rightleftharpoons}} EI^*$$

In Scheme I, inhibition involves formation of a single EI complex via a simple second-order reaction. In Scheme II, the initially formed EI complex rearranges to a stable EI* complex. To determine whether Scheme I or II represents the inhibition of fXa by rTAP, the reaction of rTAP with fXa was continuously monitored by reacting rTAP with fXa in the

presence of an indicator substrate and analyzing the time-dependent approach of the product fluorescence to its limiting slope (Zhou et al., 1989; Tian & Tsou, 1982). The pseudo-first-order rate constants describing the approach of the product concentration to its limiting value are related to the concentrations of substrate and rTAP for Schemes I and II by eq 3 and 4, respectively (Leytus et al., 1984). For Scheme

$$k_{obs} = k_1[\text{rTAP}]/(1 + [\text{S}]/K_m) + k_{-1} \quad (3)$$

$$k_{obs} = k_2[\text{rTAP}]/\{K_i(1 + [\text{S}]/K_m) + [\text{rTAP}]\} + k_{-2} \quad (4)$$

I, the pseudo-first-order rate constant for inhibition, k_{obs}, should exhibit a linear dependence on the concentration of inhibitor (eq 3), whereas for Scheme II k_{obs} should exhibit a hyperbolic dependence (eq 4, when $k_{-1} \gg k_2$), where K_i is the equilibrium constant for dissociation of the initial fXa–rTAP complex (k_{-1}/k_1) and k_{obs} is determined as described under Experimental Procedures.

Determination of the rate and equilibrium constants for reaction of rTAP with fXa from the dependence of k_{obs} on the concentration of rTAP and substrate according to eq 3 and 4 requires knowledge of K_m, the Michaelis–Menten constant, for the fXa-catalyzed hydrolysis of the substrate, S. Since reaction of fXa with excess rTAP was expected to be associated with a very low extent of conversion of the indicator substrate to product, we chose a substrate wherein low extents of conversion to products could be monitored, at values of $[\text{S}]/K_m \ll 1$, so that this term which corrects for the sequestration of the enzyme by the indicator substrate would be minimal.

The fluorogenic substrate *N-t*-Boc-Ile-Glu-Gly-Arg-7-amido-4-methylcoumarin (B-IEGR-AMC) was found suitable for use as an indicator substrate for monitoring inhibition of fXa by rTAP. The Michaelis constant, K_m, determined for this substrate, 0.75 ± 0.03 mM, is substantially higher than the previously reported value (Iwanaga et al., 1979), which was determined under different conditions in the presence of DMSO, where the concentration of DMSO increased with the substrate concentration. Control experiments (data not shown) indicated that the systematic increase in DMSO concentration was responsible for the difference between the K_m value used in the present study and the previously determined value. A value of 15 s^{-1} was determined for k_{cat} for fXa-catalyzed B-IEGR-AMC hydrolysis in a separate experiment (data not shown).

Figure 1 (inset) shows typical stopped-flow kinetic traces of the rate of hydrolysis of B-IEGR-AMC by fXa in the presence of increasing concentrations of rTAP. Pseudo-first-order rate constants for inhibition, k_{obs}, at the indicated rTAP concentrations were calculated from the kinetic traces as described under Experimental Procedures. Figure 1 illustrates the hyperbolic dependence of the measured rate constants for inhibition, k_{obs}, on the concentration of rTAP. These results exclude formation of an inhibitory fXa complex via a one-step bimolecular reaction (Scheme I). The results also exclude a slightly more complex variation of Scheme I (Scheme III) in which the inhibitor reacts via a simple second-order reaction with a slowly equilibrating conformer of the enzyme. Scheme III requires a hyperbolic decrease in k_{obs} with increasing inhibitor concentration which is inconsistent with our results (Fersht, 1985; Morrison & Stone, 1985).

Scheme III

$$E \underset{k_{-1}}{\overset{k_1}{\rightleftharpoons}} E^* + I \underset{k_{-2}}{\overset{k_2}{\rightleftharpoons}} EI^*$$

A nonlinear regression fit of the data in Figure 1 to eq 4 yielded values for K_i and k_2 of 68 ± 6 μM and 123 ± 5 s^{-1},

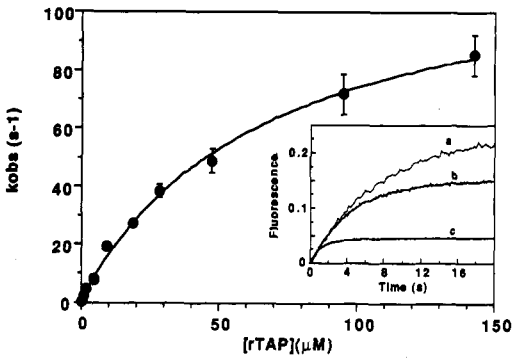

FIGURE 1: Dependence of the pseudo-first-order rate constant, k_{obs} for inhibition of fXa by rTAP on the concentration of rTAP in the presence of B-IEGR-AMC as an indicator substrate. Reactions were performed in reaction buffer at 25 °C. Solutions containing (final concentrations) B-IEGR-AMC (30 μM) and rTAP (0.05–150 μM) were mixed in the stopped-flow fluorometer with fXa (0.005–2 μM) ([fXa] ≤ 0.1[rTAP]). The fluorescence (excitation at 380 nm) was monitored using a 400-nm cutoff filter. Each value of k_{obs} represents the average of 4–8 determinations as obtained from the fit of the kinetic traces to eq 1. The error bars reflect the standard deviation of the observed values of k_{obs}. The best fit of the data to eq 4 (solid line) yields values of 123 ± 5 s^{-1} and 68 ± 6 μM for k_2 and K_i, respectively. Inset: Typical stopped-flow traces of the reaction of fXa with B-IEGR-AMC substrate. Each reaction was maintained for 8–10 half-lives of k_{obs}; concentrations of rTAP: (a) 50 nM; (b) 100 nM; (c) 500 nM.

respectively.[2] The apparent second-order rate constant (k_2/K_i) for the overall reaction is (1.8 ± 0.2) × 10^6 M^{-1} s^{-1}. Consistent with the assumption that the catalytic activity of the EI complex is near zero, a plot (data not shown) of reaction amplitude (as defined by the fluorescence change that occurred prior to attainment of the final steady-state velocity) versus the reciprocal of the inhibitor concentration was linear and intersected the *y* axis at the origin. Had the activity of EI been substantial, a measurable nonzero *y* intercept would have been observed.

Previous studies established that rTAP dissociates from fXa with a rate constant of (5.5 ± 2.0) × 10^{-4} s^{-1} (Jordan et al., 1990).[2] If rTAP inhibits fXa via Scheme II, this rate constant is equivalent to k_{-2}. Substitution of the value 5.5 × 10^{-4} s^{-1} for k_{-2} along with the values determined for K_i and k_2, and eq 5b, yields an overall equilibrium constant (as defined by eq 5a), K_i^*, of 0.30 nM for the inhibition of fXa by rTAP, which is in tolerable agreement with the value obtained in previous studies (0.18 nM; Jordan et al., 1990).

$$K_i^* = [\text{E}][\text{I}]/([\text{EI}] + [\text{EI}^*]) \quad (5a)$$

$$K_i^* = K_i[k_{-2}/(k_2 + k_{-2})] \quad (5b)$$

Reaction of rTAP with fXa in the Presence of p-Aminobenzamidine. The inhibition of fXa by rTAP was further characterized in studies using *p*-aminobenzamidine (P). This compound exhibits an enhanced fluorescence upon binding to the active site of fXa and several other trypsin-like serine proteases (Evans et al., 1982; Craig et al., 1989). Figure 2 depicts the time dependence of the change in fluorescence which occurs when a solution containing P and fXa is mixed with rTAP. The time-dependent displacement of the active-site probe P from fXa is reflected by the decrease in fluorescence in panel B which occurs between 0.5 and 60 s after mixing. Interestingly, the fluorescence is observed to increase during the first 0.5 s after mixing rTAP with a solution containing fXa and P. Since control experiments indicated that mixing

[2] The small value of k_{-2} relative to k_2 precluded accurate determination of the value of k_{-2} by fitting the data plotted in Figure 1 to eq 4.

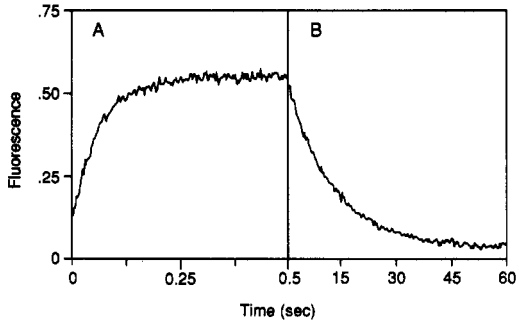

FIGURE 2: Typical stopped-flow trace for the reaction of the fXa–P complex with rTAP. The reaction was performed at 25 °C in reaction buffer with final concentrations of fXa, *p*-aminobenzamidine, and rTAP of 0.5, 100, and 5 μM, respectively. Panel A shows the increase in the fluorescence intensity of the fXa–P complex with rTAP during the first 0.5 s after mixing. Panel B shows the subsequent displacement of *p*-aminobenzamidine from the active site of fXa.

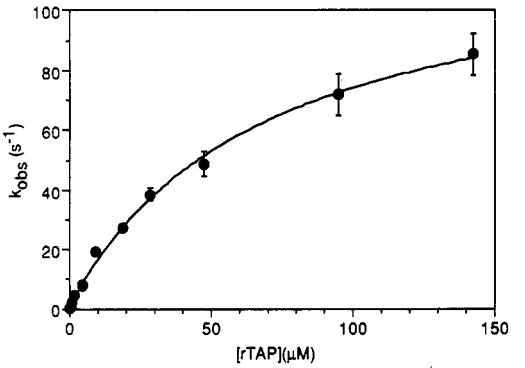

FIGURE 3: Dependence of k_{obs} for the binding of rTAP to the fXa–P complex on the concentration of rTAP. Solutions containing (after mixing concentration) fXa (0.05–0.5 μM) and P (100 μM) were mixed in a stopped-flow spectrofluorometer with rTAP (0.5–100 μM, [fXa] ≤ 0.1[rTAP]) in reaction buffer at 25 °C. Each plotted value of k_{obs} represents the average of 3–5 determinations wherein the time-dependent change in fluorescence was fit to a single exponential. The error bars reflect standard deviations. The best fit of the data to eq 6 (solid line) yields values of 143 ± 6 s^{-1} for k_2 and 39 ± 4 μM for $K_{rTAP,fXa-P}$.

rTAP with P in the absence of fXa does not result in an increase in fluorescence, the most reasonable explanation for the time-dependent increase in fluorescence depicted in panel A of Figure 2 is that rTAP binds to the fXa–P complex to form a ternary complex (fXa–P–rTAP) wherein the fluorescence of P is further enhanced. Since P binds to the active site of fXa, the rTAP in the fXa–P–rTAP complex must be interacting with a site on fXa distinct from the active site (an exosite). The rate constant for formation of this fXa–P–rTAP complex was not effected by either a 5-fold increase in ionic strength or a 4-fold increase in the concentration of P (from 100 to 400 μM; data not shown).

Rate constants for formation of the ternary complex were calculated from the pseudo-first-order approach of the fluorescence to its limiting value. Figure 3 depicts the dependence of the observed pseudo-first-order rate constant for formation of a fXa–P–rTAP complex on the concentration of rTAP. The hyperbolic dependence of the rate constant on the concentration of rTAP is most simply explained in terms of a two-step reaction pathway for the formation of the ternary complex (Scheme IV).

Scheme IV

$$\text{fXa–P} + \text{rTAP} \underset{K_{rTAP,fXa-P}}{\rightleftharpoons} \text{fXa–P–rTAP} \underset{k_{-2}}{\overset{k_2}{\rightleftharpoons}} \text{fXa–P–rTAP*}$$

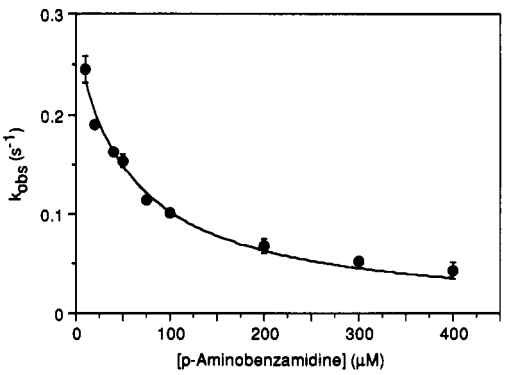

FIGURE 4: Dependence of the observed pseudo-first-order rate constant (at 25 °C) for displacement of P from fXa on the concentration of P. Solutions containing (final concentration) fXa (0.5 μM) and P (10–400 μM) were mixed in a stopped-flow spectrofluorometer with rTAP (5 μM). The fluorescence (excitation at 330 nm) was monitored using a 345-nm cutoff filter. Each point represents an average of four kinetic traces with the error bars reflecting the standard deviation of observed values. The best fit of the data to eq 7 (solid line) yields values of 61 ± 7 μM for $K_{P,fXa-rTAP*}$ and 0.27 ± 0.01 s^{-1} for k_3.

Equation 6 relates the dependence of k_{obs} on the rTAP concentration to the constants $K_{rTAP,fXa-P}$, k_2, and k_{-2}. The

$$k_{obs} = k_{-2} + k_2[\text{rTAP}]/(K_{rTAP,fXa-P} + [\text{rTAP}]) \quad (6)$$

observation that the increase in fluorescence upon mixing a buffered solution of fXa and P with a buffered solution of rTAP is a monophasic first-order process (with the fluorescence immediately following mixing being equivalent to that of a solution of fXa and P that had been mixed with buffer devoid of rTAP) is consistent with Scheme IV wherein the intrinsic fluorescence of the initial rapidly forming fXa–P–rTAP complex is equivalent to that of the fXa–P complex. A fit of the dependence of k_{obs} on [rTAP] (Figure 3) by nonlinear regression to eq 6 yielded values of 39 ± 4 μM and 143 ± 6 s^{-1} for $K_{rTAP,fXa-P}$ and k_2, respectively.[3] The equilibrium and rate constants for formation and rearrangement of the initial fXa–P–rTAP ternary complex are close to the corresponding values observed for reaction of rTAP with fXa in the absence of P. The displacement of P from the ternary complex may simply reflect a reaction pathway wherein rTAP interacts with the active site of fXa subsequent to dissociation of P from the ternary complex as depicted in Scheme V.

Scheme V

$$\text{fXa–P} + \text{rTAP} \underset{}{\overset{K_{rTAP,fXa-P}}{\rightleftharpoons}} \text{fXa–P–rTAP} \underset{k_{-2}}{\overset{k_2}{\rightleftharpoons}}$$

$$\text{fXa–P–rTAP*} \underset{}{\overset{K_{P,fXa-rTAP*}}{\rightleftharpoons}} \text{fXa–rTAP*} + \text{P} \underset{k_{-3}}{\overset{k_3}{\rightleftharpoons}} \text{fXa–rTAP**}$$

The reaction pathway depicted in Scheme V predicts that the rate constant, k_{obs}, for displacement of P from the ternary complex should decrease with increasing P, as described by eq 7, since rTAP cannot react with the active site of fXa while

$$k_{obs} = k_3 K_{P,fXa-rTAP*}/(K_{P,fXa-rTAP*} + [\text{P}]) \quad (7)$$

P is bound there. The concordance of this prediction and the experimental data is illustrated by the dependence of the pseudo-first-order rate constant for the displacement of P on the concentration of P depicted in Figure 4. A fit of the data by nonlinear regression to eq 7 yields values of 61 ± 7 μM for $K_{P,fXa-rTAP*}$ and 0.27 ± 0.01 s^{-1} for k_3. The observation that the value of k_{obs} for displacement of P by rTAP is independent of rTAP concentration up to rTAP concentrations

[3] The value of k_{-2} is too small to evaluate from the data shown in Figure 3.

of 100 μM indicates that P must be dissociating from a fXa–P–rTAP ternary complex rather than a fXa–P complex which is not complexed to rTAP (data not shown).

Determination of the Binding of rTAP to Active-Site-Blocked fXa. Further evidence that rTAP could bind to a fXa exosite was obtained in studies of the interaction of rTAP with DEGR-fXa, an active-site-blocked derivative of fXa. Although initial studies indicated that mixing rTAP with DEGR-fXa, which is itself fluorescent, yielded no change in fluorescence, kinetic evidence was obtained for the interaction of rTAP with DEGR-fXa. Preincubation of excess DEGR-fXa with rTAP followed by reaction with unmodified fXa in the presence of an indicator substrate yielded rate constants for inhibition of fXa by rTAP that decreased with increasing concentrations of DEGR-fXa. The simplest interpretation of this observation is that DEGR-fXa binds rTAP and thereby reduces the concentration of rTAP that is available for subsequent reaction with fXa. Since (as determined by control experiments) the DEGR-fXa–rTAP complex does not dissociate during the time frame used to monitor the reaction of rTAP with fXa, the rate constant (k_{obs}) for reaction of rTAP with fXa was determined by the concentration of free rTAP in solution at the end of the preincubation period.

Equation 8a (Morrison & Stone, 1985) was used to determine this rate constant for the time-dependent increase in fluorescence occurring concomitant with hydrolysis of the indicator substrate B-IEGR-AMC. V_0 and V_s are the initial,

$$F = V_s t + \{(1-\gamma)(V_0 - V_s)/\gamma k_{obs}\} \ln \{(1 - \gamma e^{-k_{obs}t})/(1-\gamma)\} + F_0 \quad (8a)$$

$$k_{obs} = k_1 K_m Q/(K_m + [S]) \quad (8b)$$

$$\gamma = (K_i^* + [fXa]_0 + [rTAP]_0 - Q)/(K_i^* + [fXa]_0 + [rTAP]_0 + Q) \quad (8c)$$

$$Q = \{(K_i^* + [fXa]_0 + [rTAP]_0)^2 - 4[fXa]_0[rTAP]_0\}^{1/2} \quad (8d)$$

uninhibited and final, inhibited velocities for substrate hydrolysis, respectively, K_i^* (0.3 nM) is the overall equilibrium constant for dissociation of the rTAP–fXa complex, $[fXa]_0$ and $[rTAP]_0$ represent the concentrations (immediately after addition of the unmodified fXa) of fXa and rTAP, respectively, K_m (0.75 mM) is the Michaelis constant for fXa-catalyzed hydrolysis of B-IEGR-AMC, and k_1 denotes the second-order rate constant for the inhibition of fXa by rTAP (k_2/K_i, Scheme II). Equation 8a assumes that the concentration of the initial EI complex of Scheme II is small relative to the concentration of free E. This approximation is valid since the concentrations of rTAP used in these experiments were at least 1000-fold below the K_i (68 μM) determined for the equilibrium constant for dissociation of the initial fXa–rTAP complex. Equation 8a takes into account the fact that a substantial fraction of the rTAP was depleted, as expressed by the γ term, in its reaction with fXa in these studies, where the concentration of free rTAP prior to reaction with fXa was of the same order of magnitude as the fXa. The value of k_1 was obtained by determining the value of k_{obs} in several control experiments wherein fXa was reacted with varying concentrations of rTAP in the absence of DEGR-fXa. The fit of the dependence of k_{obs} (determined from the fit of the data to eq 8a) on the parameter Q (the effective inhibitor concentration as defined in eq 8d) to eq 8b yielded a value of $(1.78 \pm 0.07) \times 10^6$ M^{-1} s^{-1} for k_1. This second-order rate constant is essentially identical to the value obtained from the studies described above for the reaction of fXa with a large excess of rTAP.

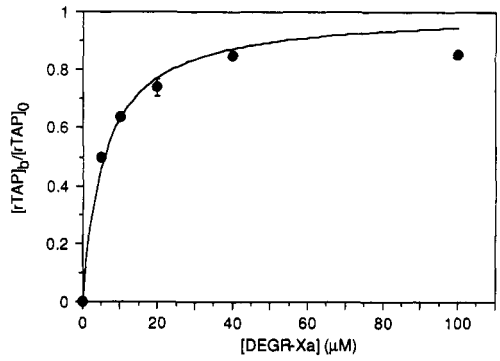

FIGURE 5: Dependence of the fraction of rTAP bound to DEGR-fXa at equilibrium on the concentration of DEGR-fXa at 25 °C. Separate mixtures of rTAP (100 nM) and DEGR-fXa (5–100 μM) were preincubated in reaction buffer for 1–4 h at room temperature. After the addition of 60 μM B-IEGR-AMC, the samples were reacted with an equal volume of 10 nM fXa in the stopped-flow fluorometer for kinetic determination of the fraction of rTAP bound to DEGR-fXa ($[rTAP]_b/[rTAP]_0$) as described in the text. The best fit of the data to eq 9 yields a value of 5.9 ± 0.7 μM for K_d.

Equations 8b and 8d were used to calculate the concentration of unbound rTAP after preincubation with DEGR-fXa from the rate constant (k_{obs}) observed for reaction of rTAP with fXa and the substrate B-IEGR-AMC at the end of the preincubation period. Figure 5 illustrates the fraction of rTAP bound to DEGR-fXa at equilibrium as a function of the concentration of DEGR-fXa. A fit of the data in Figure 5 to eq 9 (Olson & Shore, 1981) yields a value of 5.9 ± 0.7 μM

$$[rTAP]_b/[rTAP]_0 = (0.5/[T]_0) \times ([D]_0 + [T]_0 + K_d) - \{([D]_0 + [T]_0 + K_d)^2 - 4[T]_0[D]_0\}^{1/2} \quad (9)$$

for the equilibrium constant (K_d) for dissociation of rTAP from DEGR-fXa where $[rTAP]_b/[rTAP]_0$ is the fraction of rTAP bound to DEGR-fXa and $[D]_0$ and $[T]_0$ are the initial concentrations of DEGR-fXa and rTAP, respectively. Although rTAP can bind P-bound fXa and DEGR-fXa and is therefore able to bind a site distinct from the active site, the binding of rTAP to this site probably alters the interaction of the enzyme with small chromogenic substrates, since measurements with the chromogenic substrate indicate that the fXa–rTAP complex in Scheme II is essentially inactive. Further studies will be necessary to determine whether the chromogenic substrate (but not the smaller fluorescent probe P) is excluded from the active site or is bound nonproductively to the initially formed fXa–rTAP complex.

Specificity of rTAP and r-Hirudin. The similarity between the mode of action of rTAP and r-hirudin together with the fact that both enzymes are trypsin-like serine proteases prompted us to assess the possibility that rTAP and r-hirudin might weakly inhibit thrombin and fXa, respectively. The effects of these inhibitors on thrombin- and fXa-catalyzed hydrolysis of small chromogenic substrates were evaluated under conditions where $[S] \ll K_m$ so that eq 10 could be used to determine the inhibition constants (assuming competitive inhibition).

$$V_0/V_i = 1 + [I]/K_i \quad (10)$$

The linear dependencies (Figure 6) of the ratio of velocities in the absence and presence of inhibitor on inhibitor concentration yielded K_i values of 26 μM and ~3 mM[4] for the action

[4] This value of K_i should be viewed as a rough estimate, since the range of r-hirudin concentration (0–744 μM) studied was well below K_i, and the complications arising from self-association of r-hirudin (at the high r-hirudin concentrations used) have not been excluded.

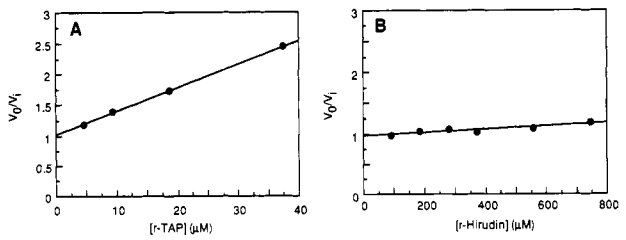

FIGURE 6: Inhibition of α-thrombin by rTAP (A) and inhibition of fXa by r-hirudin (B) in 50 mM Tris, pH 7.4, 150 mM NaCl, and 0.1% PEG 8000 using 16 μM Sar-Pro-Arg-*p*-nitroanilide (A) and 16 μM Chromozym TH (B) as substrates.

of rTAP on thrombin and r-hirudin on fXa, respectively. These values together with the K_i (0.3 nM) for the action of rTAP on fXa and the K_i (19 pM) for the action of r-hirudin on α-thrombin (Dodt et al., 1988) indicate that rTAP binds fXa (9×10^4)-fold more strongly than it binds thrombin and that r-hirudin binds thrombin ($\sim 1.6 \times 10^7$)-fold more strongly than it binds fXa.

Discussion

The results of the present study indicate that inhibition of fXa by rTAP proceeds via the two-step process described by Scheme II and that the equilibrium constant for dissociation of the initial EI complex is 68 ± 6 μM. At rTAP concentrations much less than K_i, the dependencies on rTAP concentration of the pseudo-first-order rate constant (k_{obs}) for reaction of rTAP and fXa via Scheme II (eq 4) are indistinguishable from that expected for the single one-step reaction of Scheme I (eq 3). Hence, it is not surprising that in a previous study (Jordan et al., 1990) where the rTAP concentrations were less than 20 nM, the dependence of k_{obs} on the rTAP concentration did not establish the existence of Scheme II. The observed binding of rTAP to a complex of fXa and the active-site probe *p*-aminobenzamidine indicates that rTAP can bind to a site distinct from the active site of fXa (an exosite). This behavior differs from that of the protease inhibitor antithrombin III (AT III). When a solution containing AT III is mixed with a solution containing *p*-aminobenzamidine and either fXa or thrombin, one only observes a decrease in fluorescence corresponding to displacement of *p*-aminobenzamidine from the active site of the protease (Olson & Shore, 1982; Craig et al., 1989). This observation together with the dependence of the rate constants for reaction of AT III with fXa on the *p*-aminobenzamidine concentration suggests that occupancy of the active site of fXa with P precludes reaction with AT III.

The hyperbolic dependence of rTAP concentration on the pseudo-first-order rate constant which describes the increase in fluorescence that occurs in the reaction of rTAP with fXa in the presence of *p*-aminobenzamidine indicates that binding of rTAP to the fXa–P complex is itself a two-step process which is followed by dissociation of *p*-aminobenzamidine from the active site of fXa. The value of 61 ± 7 μM observed for the equilibrium constant for dissociation of P from the ternary fXa–P–rTAP* complex ($K_{P,fXa-rTAP*}$ in Scheme V) is similar to the value of 63 ± 5 μM reported by Craig et al. (1989) for the equilibrium constant for dissociation of P from the binary fXa–P complex. Comparison of the kinetics of inhibition of fXa by rTAP in the presence and absence of P suggests that an additional slow step is introduced wherein rTAP in a rTAP–fXa complex interacts with the active site of fXa after dissociation of P from the ternary complex. The magnitude of the rate constant observed for this step (0.27 s^{-1}) is ~ 450-fold smaller than the rate constant (123 s^{-1}) observed for the slowest step in the pathway for reaction of rTAP with fXa in the absence of *p*-aminobenzamidine. These observations suggest the possibility that although rTAP can interact independently with the exosite and active site of fXa, the initial reaction of rTAP with fXa in the absence of *p*-aminobenzamidine may involve both exosite and active-site interactions. It is important to note that although formation of the most thermodynamically stable complex between rTAP and fXa is observed as a two- or three-step process, the reaction probably involves stepwise formation of numerous noncovalent interactions. It is tempting to speculate that the presence of P at the active site of fXa alters the sequence of formation of these interactions so that a new conformational rearrangement (not on the reaction pathway for inhibition of rTAP with uncomplexed fXa) must occur to form the active-site interactions that characterize the most stable complex.

The existence of a rTAP-binding exosite in fXa was confirmed by the ability of rTAP to bind to active-site-blocked DEGR-fXa. The ability of rTAP to bind to a site distinct from the active site of fXa demonstrated in the present study is the first report of the existence of a rTAP-binding exosite in fXa. The observation that the value of the overall dissociation constant (5.9 μM) for the DEGR-fXa–rTAP complex is about (3×10^4)-fold larger than the corresponding constant for the fXa–rTAP complex suggests that active-site interactions that are blocked in the DEGR-fXa–rTAP complex contribute substantially to the stability of fXa–rTAP complex. Similarly, studies of the interactions of hirudin with thrombin have shown that α-thrombin contains a hirudin-binding exosite (Stone & Hofsteenge, 1986; Chang et al., 1990; Mao et al., 1988; Maraganore et al., 1989; Naski et al., 1990) and that the 12-residue C-terminal domain of hirudin, hirugen, binds the fibrin(ogen)-binding exosite of α-thrombin. The reduced affinity of rTAP for the active-site-blocked fXa derivative, DEGR-fXa, appears to be analogous to the reduced affinity of hirudin for the active-site-blocked α-thrombin reported by Stone et al. (1987). The equilibrium constants for dissociation of native, sulfated hirudin from DIP–thrombin and PPACK–thrombin indicate hirudin binds those derivatives 10^3- and (8.6×10^5)-fold weaker than it binds native thrombin. One notable difference between the two inhibitors is that hirudin binds to the exosite of α-thrombin in an ionic strength dependent manner (Stone & Hofsteenge, 1986; Stone et al., 1989) whereas the binding of rTAP to the exosite of fXa is not affected by changes in ionic strength (0.15–0.75). Aside from this difference, the action of rTAP on fXa appears to be similar to that of hirudin on α-thrombin, with each inhibitor exhibiting a weak inhibitory activity toward the target of the other.

Acknowledgments

We thank Dr. George P. Vlasuk and Dr. Dale E. Lehman for supplying rTAP and r-hirudin, Dr. Lloyd Waxman for helpful discussions, Dr. Paul E. Bock for advice regarding the preparation of fXa, and Dr. William C. Randall for use of the stopped-flow spectrofluorometer.

References

Bock, P. E., Craig, P. A., Olson, S. T., & Singh, P. (1989) *Arch. Biochem. Biophys. 273*, 375–388.

Chang, J.-Y., Ngai, P. K., Rink, H., Dennis, S., & Schlaeppi, J.-M. (1990) *FEBS Lett. 261*, 287–290.

Craig, P. A., Olson, S. T., & Shore, J. D. (1989) *J. Biol. Chem. 264*, 5452–5461.

Di Scipio, R. G., Hermodson, M. A., & Davie, E. W. (1977a) *Biochemistry 16*, 5253–5260.

Di Scipio, R. G., Hermodson, M. A., Yates M. T., & Davie, E. W. (1977b) *Biochemistry 16*, 698–706.

Dodt, J., Kohler, S., & Baici, A. (1988) *FEBS Lett. 229*, 87-90.
Evans, S. A., Olson, S. T., & Shore, J. D. (1982) *J. Biol. Chem. 257*, 3014-3017.
Fenton, J. W., II, Fasio, M. J., Stackrow, A. B., Aronson, D. L., Young, A. M., & Finlayson, J. S. (1977) *J. Biol. Chem. 252*, 3587-3598.
Fersht, A. R. (1985) in *Enzyme Structure and Mechanism*, 2nd ed., pp 139-141, W. H. Freeman and Company, New York.
Gill, S. C., & von Hippel, P. H. (1989) *Anal. Biochem. 182*, 319-326.
Husten, E. J., Esmon, C. T., & Johnson, A. E. (1987) *J. Biol. Chem. 262*, 12953-12961.
Iwanaga, S., Morita, T., Kato, H., Harada, T., Adachi, N., Sugo, T., Maruyama, I., Takada, K., Kimura, T., & Sakakibara, S. (1979) in *Kinin II: Biochemistry, Pathophysiology, and Clinical Aspects* (Fujii, S., Mariya, H., & Suzuki, T., Eds.) pp 147-163, Plenum Press, New York.
Jordan, S. P., Waxman, L., Smith, D. E., & Vlasuk, G. P. (1990) *Biochemistry 29*, 11095-11100.
Laemmli, U. K. (1970) *Nature (London) 227*, 680-685.
Leytus, S. P., Toledo, D. L., & Mangel, W. F. (1984) *Biochim. Biophys. Acta 788*, 74-86.
Mao, S. J. T., Yates, M. T., Owen, T. J., & Krstenansky, J. L. (1988) *Biochemistry 27*, 8170-8173.
Maraganore, J. M., Chao, B., Joseph, M. L., Jablonski, J., & Ramachandran, K. L. (1989) *J. Biol. Chem. 264*, 8692-8698.
Markwardt, F. (1970) *Methods Enzymol. 19*, 924-932.
Morrison, J. F., & Stone, S. R. (1985) *Comments Mol. Cell. Biophys. 2*, 347-368.
Naski, M. C., Fenton, J. W., II, Maraganore, J. M., Olson, S. T., & Shafer, J. A. (1990) *J. Biol. Chem. 265*, 13484-13489.
Neeper, M., Waxman, L., Smith, D. E., Schulman, C., Sardana, M., Ellis, R. W., Schaffer, L., Siegl, P. K. S., & Vlasuk, G. P. (1990) *J. Biol. Chem. 265*, 17746-17752.
Olson, S. T., & Shore, J. D. (1981) *J. Biol. Chem. 256*, 11065-11072.
Olson, S. T., & Shore, J. D. (1982) *J. Biol. Chem. 257*, 14891-14895.
Sardana, M., Sardana, V., Rodkey, J., Wood, T., Ng, A., Vlasuk, G. P., & Waxman, L. (1991) *J. Biol. Chem. 266*, 13560-13563.
Stone, S. R., & Hofsteenge, J. (1986) *Biochemistry 25*, 4622-4628.
Stone, S. R., Braun, P. J., & Hofsteenge, J. (1987) *Biochemistry 26*, 4617-4624.
Stone, S. R., Dennis, S., & Hofsteenge, J. (1989) *Biochemistry 28*, 6857-6863.
Tian, W.-X., & Tsou, C.-L. (1982) *Biochemistry 21*, 1028-1032.
Warne, N. W., & Laskowski, M., Jr. (1990) *Biochemistry Biophys. Res. Commun. 172*, 1364-1370.
Waxman, L., Smith, D. E., Arcuri, K. E., & Vlasuk, G. P. (1990) *Science 248*, 593-596.
Zhou, J.-M., Liu, C., & Tsou, C.-L. (1989) *Biochemistry 28*, 1070-1076.

Isolated Oligopurine Tracts Do Not Significantly Affect the Binding of DNA to Nucleosomes†

Robert C. Getts and Michael J. Behe*
Department of Chemistry, Lehigh University, Bethlehem, Pennsylvania 18015
Received January 28, 1992; Revised Manuscript Received March 18, 1992

ABSTRACT: Nucleosomal-length DNA was constructed to contain one of two 10 bp oligopurine·oligopyrimidine sequences, either $d(A_{10}·T_{10})$ or $d(G_{10}·C_{10})$. The 146 base pair (bp) sequences were then each tandemly cloned. This allowed for the production of circularly-permuted sequence variants in which the oligopurine tract was located at eight different positions. The permuted sequences were then assayed for their ability to reconstitute into nucleosomes by competitive reconstitution. The results of the assay indicate that the free energy of nucleosome formation differs only by several tenths of a kilocalorie per mole for an oligopurine tract at any position along the DNA, including the central dyad region.

Since the great majority of DNA in a eukaryotic cell is organized into nucleosomes, the DNA sequence requirements for forming such a complex are necessarily quite nonspecific. Past experiments have shown that the nucleosome does indeed have the ability to accommodate a wide variety of DNA sequences, including prokaryotic DNA (Bryan et al., 1979), the glucosylated DNA of bacteriophage T7 (McGhee & Felsenfeld, 1982), synthetic polymers such as poly[d(A-T)]·poly[d(A-T)] (Bryan et al., 1979), poly[d(G-C)]·poly[d(G-C)] (Simpson & Künzler, 1979), poly(dG·dC) (Jayasena & Behe, 1989a,b), and poly(dA·dT) (Puhl et al., 1991), and even an RNA-DNA copolymer (Jayasena & Behe, 1989a).

There do, however, seem to be exceptional sequences which appear to deviate in either a positive or a negative direction from bulk DNA in their abilities to form nucleosomes. On the positive side, Satchwell et al. (1986) showed that there was a preference for having AA and GC dinucleotides occur with a phasing of ~10 bp, offset from each other by ~5 bp, in nucleosomal DNAs that they cloned and sequenced. Shrader and Crothers (1989, 1990), using the "rules" established by Satchwell et al. (1986), then designed synthetic polymers of the general sequence $(A/T)_3N_2(G/C)_3N_2$ and showed that they formed nucleosomes very well, with a differential free energy ($\Delta\Delta G$) of nucleosome formation significantly more favorable than bulk DNA. On the negative side, polymers that

† This work was supported by National Institutes of Health Grant GM36343.

0006-2960/92/0431-5380$03.00/0